JACS
JOURNAL OF THE AMERICAN CHEMICAL SOCIETY

Article

pubs.acs.org/JACS

Living Unimodal Growth of Polyion Complex Vesicles via Two-Dimensional Supramolecular Polymerization

Yasutaka Anraku,[†] Akihiro Kishimura,*[,†] Yuichi Yamasaki,[†] and Kazunori Kataoka*[,†,‡,§,∥]

[†]Department of Materials Engineering and [‡]Department of Bioengineering, Graduate School of Engineering, [§]Division of Clinical Biotechnology, Center for Disease Biology and Integrative Medicine, Graduate School of Medicine, The University of Tokyo, 7-3-1 Hongo, Bunkyo-ku, Tokyo 113-8656, Japan

[∥]CREST, Japan Science and Technology Agency, Sanbancho 5, Chiyoda-ku, Tokyo 102-0075 Japan

Supporting Information

ABSTRACT: Understanding the dynamic behavior of molecular self-assemblies with higher-dimensional structures remains a key challenge to obtaining well-controlled and monodispersed structures. Nonetheless, there exist few systems capable of realizing the mechanism of supramolecular polymerization at higher dimensions. Herein, we report the unique self-assembling behavior of polyion complexes (PICs) consisting of poly(ethylene glycol)-polyelectrolyte block copolymer as an example of two-dimensional supramolecular living polymerization. Monodispersed and submicrometer unilamellar PIC vesicles (nano-PICsomes) displayed time-dependent growth while maintaining a narrow size distribution and a unilamellar structure. Detailed analysis of the system revealed that vesicle growth proceeded through the consumption of unit PICs (uPICs) composed of a single polycation/polyanion pair and was able to restart upon the further addition of isolated uPICs. Interestingly, the resulting vesicles underwent dissociation into uPICs in response to mechanical stress. These results clearly frame the growth as a two-dimensional supramolecular living polymerization of uPICs.

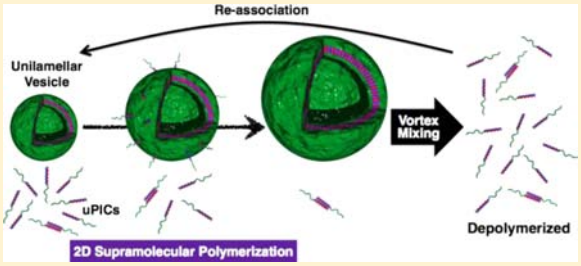

INTRODUCTION

Fabrication of self-assembled structures driven by molecular interactions (e.g., hydrophobic interactions,[1,2] electrostatic interactions,[3,4] hydrogen bonding,[5,6] and coordination bonding[7,8]) have garnered much attention, especially in constructing useful soft materials characterized by sensitivity to stimuli and reversible assembling/disassembling behavior. Although some of the many examples of self-assemblies in biological systems characterized by such dynamic behavior arise from supramolecular polymerization, only simple one-dimensional polymerization has been intensively investigated.[9] In some cases, two-dimensional (2D) supramolecular polymers were prepared, such as monolayers at interfaces, tubes, vesicles, sacs, and so forth, some of which show potential utility as functional materials.[10] Nevertheless, there has been little progress related to the supramolecular living polymerization of higher-dimensional structures, particularly those based on synthetic molecules.[11,12] One reason for such difficulty is the lack of general methods for preparing higher dimensional polymers.[10,11] In addition, the initiation and propagation steps in higher-dimensional structures are understandably difficult to control. Thus, size control of higher-dimensional structures formed by supramolecular living polymerization still presents a significant challenge.

It is assumed that 2D supramolecular polymerization occurs in systems that support spontaneous formation of layered structures. In addition, supramolecular living polymerization requires a fast initiation process, which in turn requires a monodispersed supramolecular architecture at the initial stage of the self-assembling event. To control the self-assembling behavior in a straightforward manner, we decided to exploit polyion complexes (PICs) that can be obtained in a single component solvent or aqueous medium. In fact, we demonstrated the spontaneous formation of monodispersed submicrometer-sized polyion complex vesicles (nano-PICsomes) with a narrow size distribution via the self-assembly of pairs of oppositely charged poly(ethylene glycol) (PEG)-block aniomers and homocationers in aqueous medium.[13,14] Remarkably, these nano-PICsomes exhibited a unilamellar structure, and thus, their assembly represents a novel fabrication route for well-controlled structures based on 2D supramolecular architectures. In this report, we describe the first example of 2D supramolecular living polymerization to form highly monodispersed nano-PICsomes with excellent size control. Through detailed analysis of nano-PICsome growth over time, we illustrated that the single-walled unimodal nano-PICsomes increase their size in a time-dependent manner through the dynamic 2D living assembly of unit polyion complexes (uPICs) constructed from a single polyanion/polycation pair.

Received: October 2, 2012
Published: January 4, 2013

   dx.doi.org/10.1021/ja3096587 | J. Am. Chem. Soc. 2013, 135, 1423−1429

RESULTS AND DISCUSSION

Unimodal Growth of Nano-PICsomes. Monodispersed nano-PICsomes 100 nm in diameter (polydispersity index (PDI) < 0.1) were prepared as previously reported by mixing oppositely charged PEG-block aniomers (PEG-P(Asp)) and homocatiomers (homo-P(Asp-AP) in aqueous medium.[13] Notably, we found that, by increasing the temperature from 4 to over 15 °C, the nano-PICsomes grew continuously over time as observed by dynamic light scattering (DLS). At a total polymer concentration of 1 mg/mL, vesicle sizes gradually increased from 100 to 280 nm and reached a plateau over ∼2 days while maintaining their initial monodispersity (PDI < 0.1; Figure 1a,b). The highly monodispersed size distribution was confirmed by histogram analysis of DLS results (Figure 1c), and the vesicles maintained a unilamellar structure of thickness of approximately 10−15 nm (Figure 1d−f). Nano-PICsomes with varying initial diameters prepared by varying the polymer concentration between 0.1 and 3 mg/mL were tracked over time by DLS. We observed an increased growth rate with increasing concentration (see the Supporting Information, Figure S1) ranging from 0.5 to 3 mg/mL, yet growth was negligible at the lowest examined concentration (0.1 mg/mL). Subsequently, we focused on the system obtained at the polymer concentration of 1 mg/mL as a representative case.

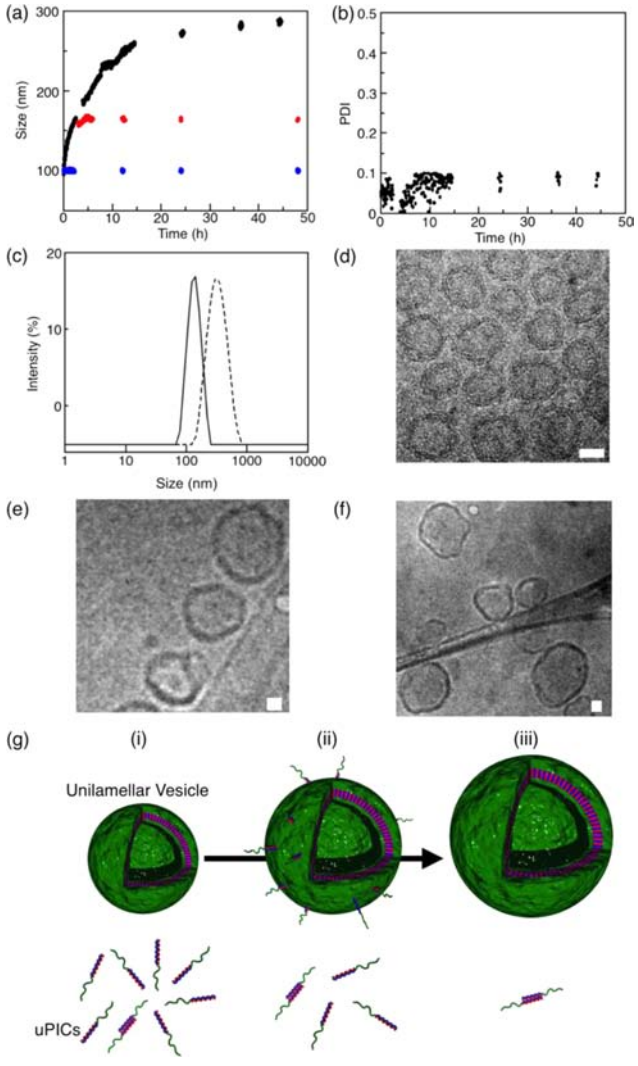

Figure 1. (a) Time-dependent growth of un-cross-linked (black) and cross-linked nano-PICsomes (blue: cross-linking just after preparation; red: cross-linking 3 h after preparation) as determined by DLS. Total polymer concentration was 1 mg/mL. (b) Time dependence of PDI of nano-PICsomes. (c) Particle size distributions of nano-PICsomes (1 mg/mL). The solid line shows data taken just after preparation, while the dashed line shows data taken at day 2 as determined by DLS. (d−f) Representative cryo-transmission electron microscopy (cryo-TEM)[15−17] images of nano-PICsomes after cross-linking treatment: d, 0 h; e, 5 h; f, 24 h. Scale bar is 50 nm. The white dashed line shows a contour of the microgrid. (g) The proposed mechanism of growth of nano-PICsomes.

Mechanism Involved in the Growth of Nano-PICsomes. The most plausible mechanisms underlying the unique growth behavior of the unilamellar PIC vesicles include simple vesicle fusion and a phenomenon known as Ostwaldt ripening, which involves redeposition of components from smaller to larger particles.[18] Nevertheless, both vesicle fusion and Ostwald ripening typically result in the broadening of the vesicle size distribution, which is inconsistent with the observation of monodispersive vesicle growth reaching a plateau over time. Moreover, vesicle fusion during growth was clearly ruled out by a study described below using fluorescence cross-correlation spectroscopy (FCCS) and PICsomes loaded separately with Cy5- and FITC-labeled dextran (M_r = 40 000).

As seen in Figure 2, the autocorrelation curves of Cy5 and FITC from the mixture of Cy5−dextran-loaded and FITC−dextran-loaded nano-PICsomes are consistent with the previously reported curves of PICsomes[13] showing their growth over time (see the Supporting Information, Table S1). Nevertheless, no cross-correlation between Cy5 and FITC was observed, as indicated by the black solid line in Figure 2; this remained the case even 3 days after mixing. This result indicates that Cy5−dextran and FITC−dextran diffuse totally independently without any mixing in the same nano-PICsome compartment, thereby eliminating the possibility of vesicle fusion during the growth process.

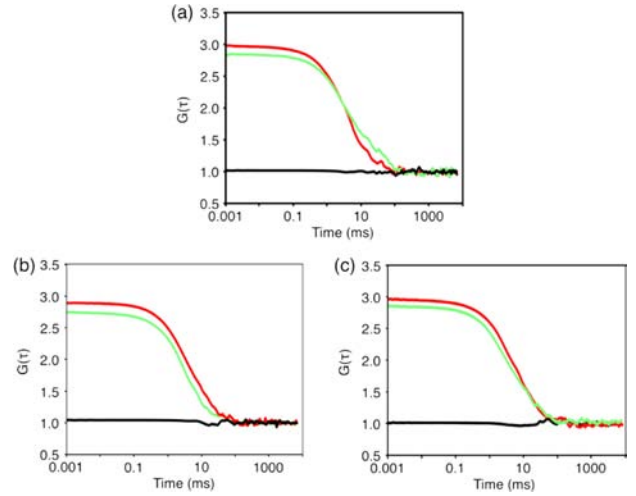

Figure 2. (a−c) Time dependency of cross-correlation curves (black line) and autocorrelation curves (green and red lines) of a mixture of Cy5−dextran-loaded nano-PICsomes and FITC−dextran-loaded nano-PICsomes. The green line indicates Cy5 fluorescence, and the red line indicates FITC fluorescence: (a) just after mixing; (b) 1 day after mixing; and (c) 3 days after mixing.

dx.doi.org/10.1021/ja3096587 | J. Am. Chem. Soc. 2013, 135, 1423−1429

Next, to get insight into the growth mechanism of uniform vesicles, snapshot analysis during the growth of nano-PICsomes was carried out by in situ cross-linking of PICs by adding 1-ethyl-3-(3-dimethylaminopropyl) carbodiimide hydrochloride (EDC) to the solution at various time points.[13] Nano-PICsomes showed no growth after EDC treatment (red and blue closed circles in Figure 1a), in contrast to un-cross-linked nano-PICsomes that grew over the course of ∼2 days; this indicates that the structure of nano-PICsomes could be successfully captured and fixed at any particular moment. Figure 3a shows the size-exclusion chromatography (SEC)

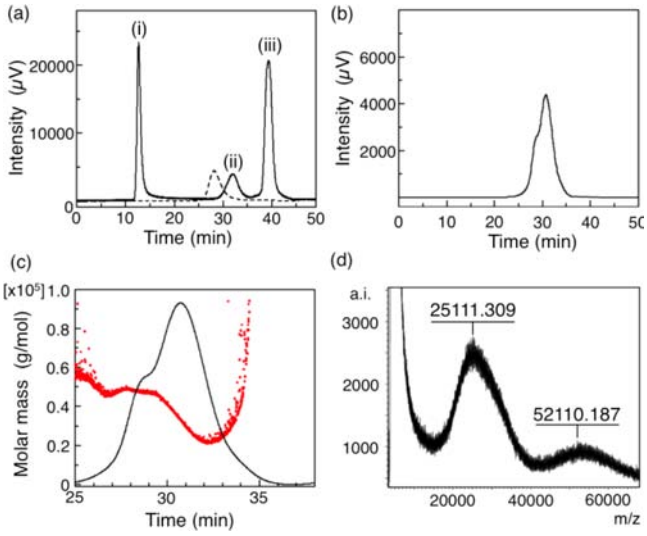

Figure 3. SEC traces of cross-linked nano-PICsomes and isolated PICs. (a) SEC traces of cross-linked nano-PICsomes just after preparation (solid line) and of PEG-P(Asp) (dashed line). (b) SEC trace of isolated PICs. (c) SEC trace of isolated PICs (black line) and MALLS profile (red line). (d) MALDI-TOF mass spectrum of isolated PICs.

results of the fixed nano-PICsome solution immediately after preparation. Here, peak i at the exclusion limit corresponds to the cross-linked nano-PICsomes, while peak iii corresponds to derivatives from the cross-linking reagent. Since free polymer, PEG-P(Asp), eluted at a retention time of ∼30 min (Figure 3a, dashed line), it was not possible that peak ii corresponded to the free polymer. The fraction containing peak ii was isolated by filtration (molecular weight cutoff (MWCO): 300 000 and 3000), and the structure was analyzed using SEC-multiangle laser light scattering (SEC-MALLS) and matrix-assisted laser desorption/ionization time-of-flight mass spectrometry (MALDI-TOF MS). Successful isolation of the peak ii fraction was confirmed by SEC as shown in Figure 3b. From the MALLS data (red line) superimposed on the SEC trace (black line) in Figure 3c, the molecular masses of the compounds corresponding to the shoulder (∼27 min) and the peak (∼31 min) in the SEC trace were determined to be approximately 50 000 and 25 000 g/mol, respectively. These values were corroborated by the MALDI-TOF MS result, shown in Figure 3d. As PEG-P(Asp) and homo-P(Asp-AP) have molecular weights of 12 500 and 11 000, respectively, the major fraction of peak ii (M_r ∼ 25 000) is likely to be a single PEG-P(Asp)/homo-P(Asp-AP) pair, defined here as a uPIC, with a minor fraction of dimer uPIC (M_r ∼ 50 000) appearing as the shoulder at ∼27 min in the SEC trace. In fact, peak separation analysis revealed that uPICs accounted for approximately 83% of the total area of the peak ii fraction (Supporting Information, Figure S2 and Table S2). This supports the hypothesis that uPICs play an active role in the unimodal growth of the nano-PICsome 2D assembly over time through the irreversible insertion of uPICs into the seed nano-PICsomes.

This hypothesis was further probed through a series of fluorescent labeling experiments (Figure 4). First, Cy3-labeled nano-PICsomes, assembled from Cy3-labeled PEG-P(Asp) (PEG-P(Asp)-Cy3) and homo-P(Asp-AP), and unlabeled nano-PICsomes of nearly the same size were prepared. Then, uPICs (including some fraction of dimer uPICs) in the nano-PICsome solution were separated by ultrafiltration (MWCO = 300 000) as confirmed by SEC (Figure 4a). The isolated Cy3-labeled uPICs were then added to the uPIC-free, unlabeled nano-PICsome solution, followed by cross-linking at designated times (0, 1, and 24 h) and monitoring via SEC using both a UV detector (220 nm) and a fluorescence detector (FP detector, Ex/Em = 520/550 nm; Figure 4c). Just after mixing, the SEC trace generated by UV absorption showed two peaks corresponding to the nano-PICsomes and uPICs (see the Supporting Information, Figure S3), while fluorescence was detected only in the uPIC fraction (Figure 4c-i). Notably, after 1 h of incubation, there emerged fluorescence at the peak position corresponding to the nano-PICsomes (Figure 4c-ii); the fluorescence intensity of this peak appreciably increased at 24 h (Figure 4c-iii). This trend was clearly inversely correlated with a decrease in the fluorescence intensity of the uPIC peak over time (Figure 4c-ii, -iii) and evaluated in detail by UV absorption monitoring (Supporting Information, Figures S3). It is thus reasonable to conclude that uPIC integration into the nano-PICsome membrane caused a continuous increase in the surface area, driving the unimodal growth of the nano-PICsome. On the other hand, the suppression of growth observed at the lowest polymer concentration (Supporting Information, Figure S1) can be accounted for by the very small amount of uPIC initially formed in the solution (Supporting Information, Table S3 and Figure S4).

To further clarify the dynamics of uPIC interactions with nano-PICsomes, isolated unlabeled uPICs were added to the uPIC-free Cy3-labeled nano-PICsome solution (Figure 4b). Interestingly, the fluorescence peak corresponding to the uPICs was not found in the SEC trace even after the completion of vesicle growth (Figure 4d), implying that release of Cy3-labeled uPICs from the nano-PICsomes did not occur. Taken together, these observations demonstrate that nano-PICsome growth caused by the integration of uPICs was essentially a one-way process. This phenomenon constitutes a new class of supramolecular polymerization, in which uPICs as an active species are directed exclusively into the 2D assembly of vesicle structures (Figure 1g). The nano-PICsome solution initially contained both seed nano-PICsomes (∼100 nm) and uPICs (including the minor dimer fraction; Figure 1g-i). The initial assembly of uPICs into 2D lamellae may proceed very rapidly to compensate for the significant interfacial energy at the lamellar edge, resulting in the closure of lamella into vesicle structures, that is, seed nano-PICsome formation, as we reported previously.[13] Following this fast initiation step, the slow propagation consisting of the insertion of remaining uPICs into the seed nano-PICsomes induced their growth in a regulated manner. It is worth noting that uPIC integration into nano-PICsomes was energetically favorable, with an activation energy of 40.4 kJ/mol (vide infra; Supporting Information,

dx.doi.org/10.1021/ja3096587 | J. Am. Chem. Soc. 2013, 135, 1423−1429

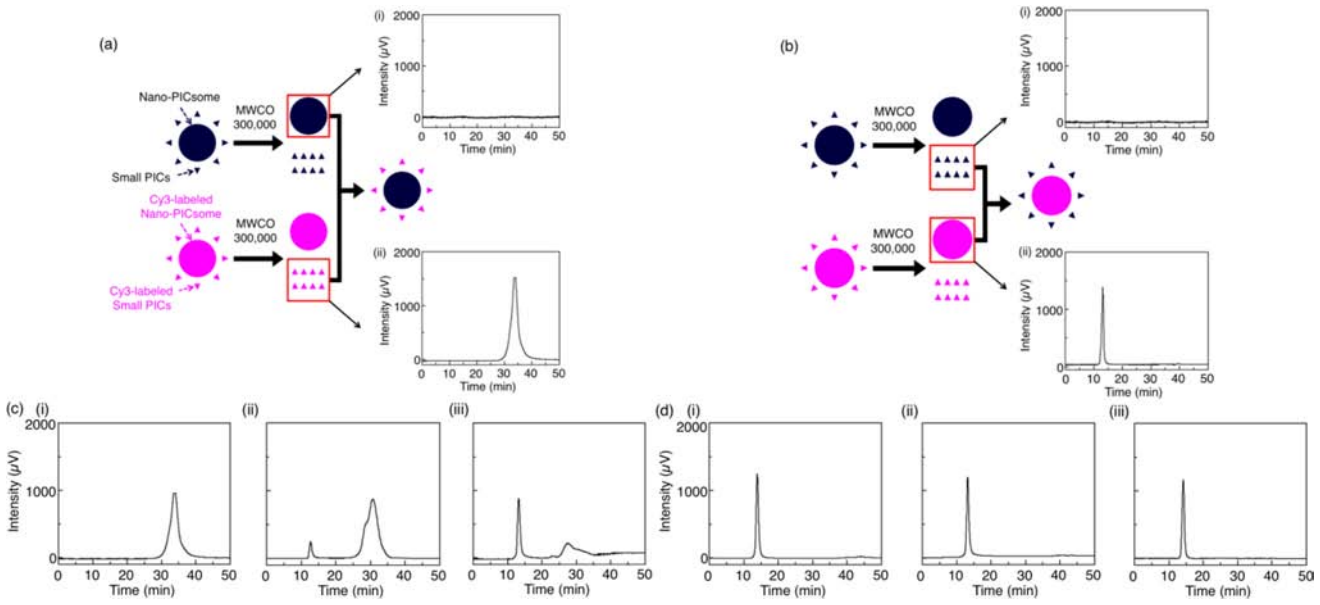

Figure 4. (a) Experimental concept of mixing unlabeled nano-PICsomes with Cy3-labeled small PICs and (b) mixing Cy3-labeled nano-PICsomes with unlabeled small PICs. SEC traces of (a-i) isolated unlabeled nano-PICsomes, (a-ii) isolated small Cy3-labeled PICs, (b-i) isolated unlabeled PICs, and (b-ii) isolated Cy3-labeled nano-PICsomes were recorded using a fluorescent detector (Ex/Em = 520/550 nm). (c–d) Time-dependent composition changes of PICs were recorded using a fluorescent detector (Ex/Em = 520/550 nm), corresponding to (c) panel a and (d) panel b. The mixture of isolated unlabeled nano-PICsomes and Cy3-labeled small PICs were analyzed at (c-i) 0 h, (c-ii) 1 h, and (c-iii) 24 h after cross-linking by EDC. The mixture of isolated unlabeled small PICs and Cy3-labeled nano-PICsomes was analyzed at (d-i) 0 h, (d-ii) 1 h, and (d-iii) 24 h after cross-linking by EDC. SEC traces recorded using a UV detector (220 nm) are shown in the Supporting Information, Figure S3.

Figure S6c), despite the presence of a sterically stabilized PEG layer on the surface (Figure 1g-ii). The minor dimer fraction of uPICs appears dormant in this propagation step, as the SEC peak corresponding to the dimer (and perhaps a small amount of higher aggregates) remained even at the termination of vesicle growth (Figures 4c-iii, and S5, Supporting Information). Presumably, higher aggregates of uPIC cannot directly integrate into the PIC lamellae of the vesicle and eventually behave as dormant species.

Given that pure uPICs (without dimer and higher aggregates) were the only active species, the growth curve of the vesicles was expected to follow first-order kinetics. According to the method described in the Supporting Information, kinetic analysis of the vesicle growth was done based on the data shown in Figure 1. Briefly, Table S4 of the Supporting Information shows a portion of the nano-PICsome growth data as a function of time. As mentioned above, nano-PICsomes possess a unilamellar structure with a definite particle size at any time point t (Figure 1a–f). Thus, the square of the average diameter (d^2) should be proportional to the number of molecules incorporated within the nano-PICsome membrane at any t. Assuming that active species A (= uPIC) is the only source for size growth, we can approximate the concentration of A at time t as

$$[\mathrm{A}]_t = [\mathrm{A}]_0 - 4\pi\nu N[\{d(t)\}^2 - \{d(0)\}^2]/V \quad (1)$$

where $[\mathrm{A}]_t$ is the concentration of A as a function of time, $[\mathrm{A}]_0$ is the initial concentration of A, ν is the number density of A in a PIC layer of a nano-PICsome, N is the number of vesicles, and V is the volume of the solution. In this study, ν, N, and V were assumed to be constant. Therefore, given a first-order rate law governing nano-PICsome formation, a plot of $\ln[\mathrm{A}]_0/[\mathrm{A}]_t$ versus t was expected to yield a linear fit using the least-squares method, which was borne out (Figure 5c). In fact, the time

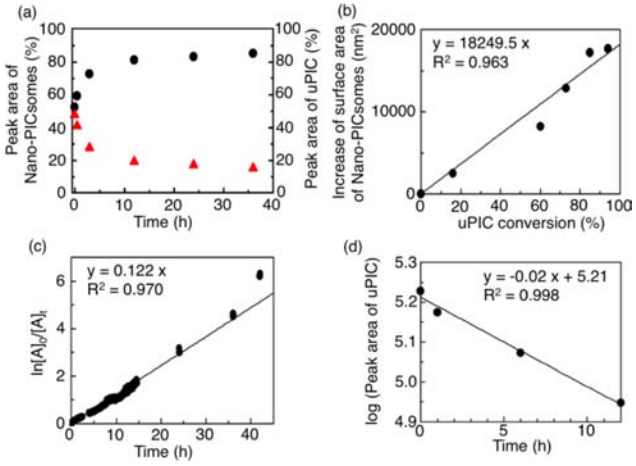

Figure 5. (a) Growth of nano-PICsomes (black curve) and consumption of uPICs (red curve) was evaluated based on peak areas of SEC chromatograms. SEC traces were recorded using a fluorescent detector (Ex/Em = 520/550 nm). (b) Relationship between uPIC conversion and increase in surface area of PICsomes at specific time points. The fitting curve was obtained using a least-squares method. (c) Plot of analysis time against $\ln[\mathrm{A}]_0/[\mathrm{A}]_t$, where [A] is the concentration of uPICs, was calculated from the change in size based on DLS analysis. (d) Plot of uPIC consumption against time.

dependency of A (uPIC) consumption is quite consistent with first-order kinetics (Figure 5a,d). The peak area corresponding to the uPICs was reduced to approximately 20% of its maximum value at the termination of growth, which corresponds to the amount of dimer uPICs found at the initial stage (Supporting Information, Figure S2 and Table S2). These results strongly support that only uPICs act as active species in the system.

dx.doi.org/10.1021/ja3096587 | J. Am. Chem. Soc. 2013, 135, 1423–1429

More interestingly, this supramolecular polymerization exhibited living polymerization character. We observed that vesicle sizes remained constant when uPICs were removed from the un-cross-linked nano-PICsome solution (Figure 6a).

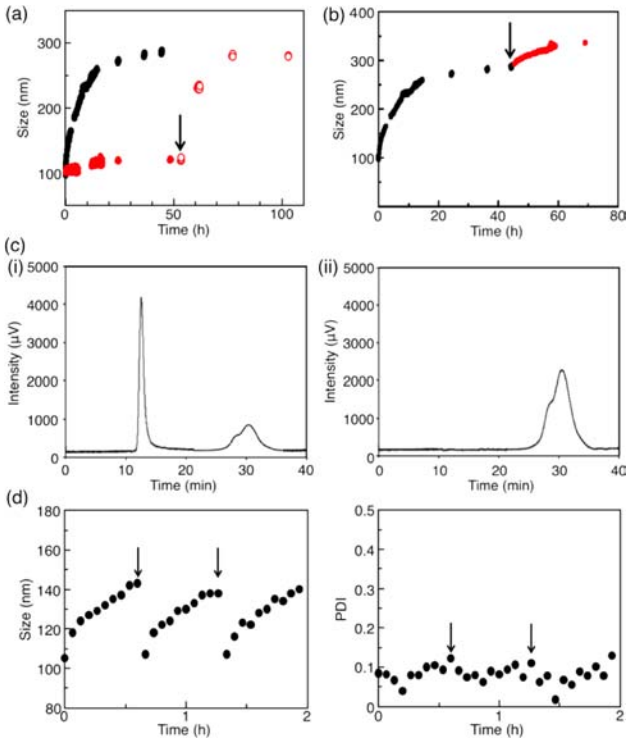

Figure 6. (a) Time dependency of nano-PICsome size before (black dots) and after (red dots) removal of small PICs followed by the addition of uPICs (red circles). Time points at which uPICs were added are marked with arrows. The total polymer concentration was 1 mg/mL. Time dependency of the PDI is shown in the Supporting Information. (b) Time dependency of nano-PICsome size before (black dots) and after (red dots) addition of additional uPICs. Time points at which uPICs were added are marked with arrows. The initial total polymer concentration was 1 mg/mL. The sizes of nano-PICsomes were determined by DLS. (c) Composition of PICs before (i) and after (ii) application of shear stress (vortex mixing). SEC traces of PICs cross-linked immediately after preparation (i) and during vortex mixing (ii). (d) Responses of PICsomes to shear stress. Time-dependent changes in size were observed by DLS (right: size; left: PDI). The time points at which shear stress was applied to the system are marked with arrows. The total polymer concentration was 1 mg/mL.

However, a growth profile identical to that of the original solution was observed when the separated uPICs were added again to the nano-PICsome solution. If additional uPICs were added to a solution of mature nano-PICsomes that had reached the saturated size (280 nm) due to consumption of the original uPICs, further size growth was clearly observed (Figure 6b). This result reveals that nano-PICsomes remained active species for growth as long as the supply of uPICs persisted. In addition, uPIC conversion was roughly proportional to the increase in the nano-PICsome surface area, which is linearly correlated with the apparent total number of polymers contained in the PIC lamellae (Figure 5b). The behaviors of supramolecular polymerization of uPICs into nano-PICsomes, including first-order kinetics, have an apparent similarity to elemental processes in chain reactions forming covalent bonds without definite termination, a typical example of which is the living polymerization of vinyl monomers. The formation of monodispersed seed nano-PICsomes at the initial stage may correspond to the fast initiation step, followed by the slow propagation step of uPIC insertion into the PIC membrane. Recurrence of nano-PICsome growth by additional uPICs reflects the living nature of the process up to the maximum size measurable in this experiment (~300 nm). To the best of our knowledge, this is the first example of 2D supramolecular living polymerization using synthetic macromolecules.

Temperature Dependence of Nano-PICsome Growth. Although it was possible that residual charge remained in the uPICs due to small imbalances in the charged segment length of the block aniomer (DP = 75)/homocatiomer pair (DP = 82), charge neutralization accompanied by the release of the majority of the small counterions significantly reduced the hydration of PIC moieties in block aniomer/homocatiomer pairs (uPICs), driving their insertion into PICsomes to compensate for the interfacial free energy. Segregation of PEG strands from PIC domains due to their immiscible nature led to the formation of the three-layered membrane structure of the nano-PICsomes, consisting of an inner PIC phase sandwiched by external and internal PEG layers.[13] It is of interest that uPICs could insert into the inner PIC phase of nano-PICsomes, crossing the steric barrier of the external PEG layer. Furthermore, translocation of PEG-PAsp into nano-PICsomes from the external to internal sides should occur during the growing process so as to balance the PEG density on both sides of the PIC membrane. Thus, the membrane of nano-PICsomes is likely to be highly dynamic with appreciable lateral mobility of constituent polyelectrolytes.

To obtain further insight into the dynamic features of nano-PICsome membranes, temperature dependency was carefully examined. Nano-PICsome growth curves were recorded at various temperatures (4, 20, 23, 25, and 35 °C; Supporting Information, Figure S6). Growth was clearly accelerated by an increase in temperature, particularly within the range between 20 and 35 °C, suggesting that the supramolecular polymerization was an endothermic reaction. Attaining the final size of approximately 280 nm over this temperature range corresponded to the consumption of all the free uPICs in the solution regardless of the reaction temperature. The Arrhenius plot obtained from the growth curves at different temperatures allowed us to calculate the activation energy of uPIC integration into the nano-PICsome membrane as 40.4 kJ/mol. This is approximately 15 times greater than the thermal energy at room temperature, ~2.5 kJ/mol at 300 K. It may be of interest to note that this is one-third of the activation energy required for the propagation step of the assembly of type I collagen fibrils, 113 kJ/mol, which is a typical example of entropy-driven supramolecular polymerization in biological systems.[19] In sharp contrast with temperature-correlated growth observed at ≥20 °C, the fact that no growth was observed at 4 °C (Supporting Information, Figure S6a) was unexpected and was certainly not in line with the Arrhenius plot generated from data collected at ≥20 °C. A discrete change in the PIC membrane properties, most probably decreased mobility, may occur between 4 and 20 °C, quenching uPIC integration into nano-PICsomes. Further investigation is required, the results of which will be reported in the near future.

Reversible Association/Dissociation of PICsomes in Response to Shear Stress. As described, uPIC integration

dx.doi.org/10.1021/ja3096587 | J. Am. Chem. Soc. 2013, 135, 1423−1429

into nano-PICsomes, defined here as supramolecular polymerization, is essentially a one-way process without any sign of depolymerization as ascertained by the fact that no uPICs released from the nano-PICsomes were observed (Figure 4) and that PICsome size remained constant even after the removal of uPICs (Figure 6a). Notably, 100-fold dilution did not induce any change in the size observed using DLS (data not shown), indicating that PICsomes did not undergo spontaneous dissociation or size reduction. Nevertheless, it is worth noting that the apparently stable supramolecular PICsome system easily underwent depolymerization into uPICs upon application of mild mechanical stress in the form of 2 min of vortex mixing. This was directly evidenced by adding the cross-linking reagent EDC into the PICsome solution during vortex mixing to capture the existing components under shear stress. As seen in Figure 6c, only the peak corresponding to uPICs, with no PICsome peak, was observed in the SEC trace of the EDC-treated solution that underwent vortex mixing. Interestingly, the peak area was nearly identical to the sum of the peak areas corresponding to the nano-PICsomes and uPICs in the original solution (Supporting Information, Table S5), indicating that the shear stress-induced depolymerization of nano-PICsomes into uPICs occurred quantitatively. Furthermore, termination of vortex mixing instantaneously caused the reformation of nano-PICsomes with the identical size and size distribution of the original system in a reproducible manner (Figure 6d), demonstrating the rapid assembly process of uPICs into nano-PICsomes under static conditions. These rapid initialization and reformation processes are quite consistent with our previous report, in which we proposed that the initial nano-PICsome is likely to emerge rapidly in a confined unit space of constant volume within the solution, thereby leading to the formation of monodisperse vesicles.[13] The sensitive response against shear stress observed here is quite unique, and PIC elements in nano-PICsomes may form a correlated structure with less entanglement in the membrane that produces a dynamic response against external forces while maintaining appreciable stability under force-free conditions.

As discussed in our previous report, the PIC system reported here exhibits a critical concentration of around 0.09 mg/mL, below which no fraction with the size of ∼100 nm was observed.[13] After vortex mixing of a diluted nano-PICsome solution at a concentration of 0.05 mg/mL, there was no reformation of nano-PICsomes, and the solution contained only uPICs (Supporting Information, Figure S8). Consistent with this observation, PIC initially prepared at 0.05 mg/mL contained only uPICs, even after 48 h (Supporting Information, Figures S9−11). These results clearly show that uPICs are monomer elements of this supramolecular polymerization that initiates above the critical concentration of ∼0.09 mg/mL. The detailed mechanism involved in this fast initiation step is yet to be characterized and merits further investigation.

CONCLUSION

In summary, we demonstrated the growth process of PICsomes consisting of block aniomer and homocatiomer pairs through the one-way integration of the minimum PIC unit (uPIC). The growth began with a fast initiation process, that is, the prompt formation of seed PICsomes of homogeneous size, followed by the relatively slow but irreversible propagation step of uPIC insertion into the seed PICsomes; this propagation induced continuous increase in their size while maintaining their monodispersity until the feed uPICs were completely consumed. The resulting PICsomes were dormant in the absence of uPICs, but recurrent growth was observed upon feeding additional uPICs into the medium. These propensities of continuous growth without termination have similarities to living polymerization, and the process can be framed as a supramolecular living polymerization in a 2D system, which was to the best of our knowledge, the first reported instance of such a phenomenon. The "living" nature of the PIC self-assembly may allow for further installation of functional components or different types of uPICs into the original assembly in a well-controlled manner. Furthermore, the reversible assembly/disassembly of PICsomes was induced by the application of external shear stress. This sensitive response to external force gives PICsomes potential utility as functional smart materials with diverse applications, such as self-healing materials, in addition to granting further insight into the correlated structure of single-layered PICs with dynamic properties. Additionally, the dynamic properties of PICs are highly dependent on the nature of their constituent uPICs. Design of uPICs and control of their behavior may lead to the development of advanced soft materials, achieving both specific environmental sensitivity and toughness against nonspecific external stimuli utilizing PIC architectures.

ASSOCIATED CONTENT

Supporting Information

Additional information as noted in the text. This material is available free of charge via the Internet at http://pubs.acs.org.

AUTHOR INFORMATION

Corresponding Author

kishimura@bmw.t.u-tokyo.ac.jp; kataoka@bmw.t.u-tokyo.ac.jp

Notes

The authors declare no competing financial interests.

ACKNOWLEDGMENTS

This research was supported in part by a Grant-in-Aid for Scientific Research (Nos. 21106505 and 23106705 to A.K. and 20·10495 to Y.A.) from the Ministry of Education, Culture, Sports, Science, and Technology (MEXT) of Japan, the Core Research Program for Evolutional Science and Technology from the Japan Science and Technology Agency, and by the Japan Society for the Promotion of Science (JSPS) through the "Funding Program for World-Leading Innovative R&D on Science and Technology (FIRST Program)," initiated by the Council for Science and Technology Policy (CSTP). We are grateful to Drs. A. Kitayama and S. Sugitani, Terabase Inc., for cryo-TEM images. Y.A. thanks the JSPS Research Fellowship for Young Scientist. A.K. thanks the Kao Foundation for Arts and Sciences and the Izumi Science and Technology Foundation for financial support.

REFERENCES

(1) Zhang, L.; Eisenberg, A. *Science* **1995**, *268*, 1728−1731.
(2) Battaglia, G.; Ryan, A. J. *Macromolecules* **2006**, *39*, 798−805.
(3) Harada, A.; Kataoka, K. *Science* **1999**, *283*, 65−67.
(4) Koide, A.; Kishimura, A.; Osada, K.; Jang, W. D.; Yamasaki, Y.; Kataoaka, K. *J. Am. Chem. Soc.* **2006**, *128*, 5988−5989.
(5) Ilhan, F.; Galow, T. H.; Gray, M.; Clavier, G.; Rotello, V. M. *J. Am. Chem. Soc.* **2000**, *122*, 5895−5896.
(6) Yoshikawa, I.; Sawayama, J.; Araki, K. *Angew. Chem., Int. Ed.* **2008**, *47*, 1038−1041.

(7) Osada, K.; Cabral, H.; Mochida, Y.; Lee, S.-E.; Nagata, K.; Matsuura, T.; Yamamoto, M.; Anraku, Y.; Kishimura, A.; Nishiyama, N.; Kataoka, K. *J. Am. Chem. Soc.* **2012**, *134*, 13172−13175.
(8) Li, D.; Zhang, J.; Landskron, K.; Liu, T. *J. Am. Chem. Soc.* **2008**, *130*, 4226−4227.
(9) de Greef, T. F. A.; Smulders, M. M. J.; Wolffs, M.; Schenning, A. P. H. J.; Sijbesma, R. P.; Meijer, E. W. *Chem. Rev.* **2009**, *109*, 5687−5754.
(10) Sakamoto, J.; van Heijst, J.; Lukin, O.; Schluter, A. D. *Angew. Chem., Int. Ed.* **2009**, *48*, 1030−1069.
(11) Gilroy, J. B.; Gädt, T.; Whittell, G. R.; Chabanne, L.; Mitchels, J. M.; Richardson, R. M.; Winnik, M. A.; Manners, I. *Nat. Chem.* **2010**, *2*, 566−570.
(12) Gädt, T.; Schacher, F. H.; McGrath, N.; Winnik, M. A.; Manners, I. *Macromolecules* **2011**, *44*, 3777−3786.
(13) Anraku, Y.; Kishimura, A.; Oba, M.; Yamasaki, Y.; Kataoka, K. *J. Am. Chem. Soc.* **2010**, *132*, 1631−1636.
(14) Anraku, Y.; Kishimura, A.; Kobayashi, A.; Oba, M.; Kataoka, K. *Chem. Commun.* **2011**, *47*, 6054−6056.
(15) Hosokawa, F.; Danev, R.; Arai, Y.; Nagayama, K. *J. Electron Microsc.* **2005**, *54*, 317−324.
(16) Danev, R.; Nagayama, K. *Ultramicroscopy* **2001**, *88*, 243−252.
(17) Sugitani, S.; Nagayama, K. *J. Phys. Soc. Jan.* **2002**, *71*, 744−756.
(18) Sugimoto, T. *Monodispersed Particles*; Elsevier: Amsterdam, the Netherlands, 2001; pp 140−144.
(19) Kadler, K. E.; Hojima, Y.; Prockop, D. J. *J. Biol. Chem.* **1988**, *263*, 10517−10523.